INORGANIC CATIONS IN RAT KIDNEY

Localization with Potassium Pyroantimonate–Perfusion Fixation

C. J. TANDLER and A. L. KIERSZENBAUM

From the Instituto de Anatomía General y Embriología, Facultad de Medicina, and the Centro de Investigaciones sobre Reproducción, Facultad de Medicina, Buenos Aires, Argentina

ABSTRACT

For localization of pyroantimonate-precipitable cations, rat kidney was fixed by perfusion with a saturated aqueous solution of potassium pyroantimonate (pH about 9.2, *without* addition of any conventional fixative). A remarkably good preservation of the tissue and cell morphology was obtained as well as a consistent and reproducible localization of the insoluble antimonate salts of magnesium, calcium, and sodium. All proximal and distal tubules and glomeruli were delimited by massive electron-opaque precipitates localized in the basement membrane and, to a lesser extent, in adjacent connective tissue. In the intraglomerular capillaries the antimonate precipitate was encountered in the basement membranes and also between the foot processes. In addition to a more or less uniform distribution in the cytoplasm and between the microvilli of the brush border, antimonate precipitates were found in all cell nuclei, mainly between the masses of condensed chromatin. The mitochondria usually contained a few large antimonate deposits which probably correspond to the so-called "dense granules" observed after conventional fixations.

INTRODUCTION

Although inorganic ions are essential constituents of all animal and plant tissues, relatively little is yet known about their distribution as they exist in the living cell. Recently, the localization of the cations magnesium, calcium, and sodium (1, 2), as well as that of inorganic orthophosphate anions (3, 4), was revealed by electron microscope and microprobe analysis with the use of, respectively, potassium pyroantimonate and lead acetate aqueous solutions as fixatives.

Although potassium pyroantimonate was first employed mixed with osmium tetroxide (5, 6)—a procedure basically followed by all subsequent investigators (7–23)—Tandler et al. (1, 2) were the first to show that this salt *alone* behaves as a fixative and, furthermore, that the antimonate precipitates contained magnesium and calcium in addition to sodium.

In the present paper we demonstrate that perfusion with an aqueous saturated solution of potassium pyroantimonate offers a definitive advantage over the immersion technique employed before (1, 2), in that the tissue showed a remarkably good preservation at the ultrastructural level. Because of the high level of inorganic cations associated with the basement membranes in mouse testis (2) and within the cell nucleus (1, 2), a similar accumulation of cations was expected for other tissues too. The evidence presented here demonstrates that this is indeed the case for rat kidney.

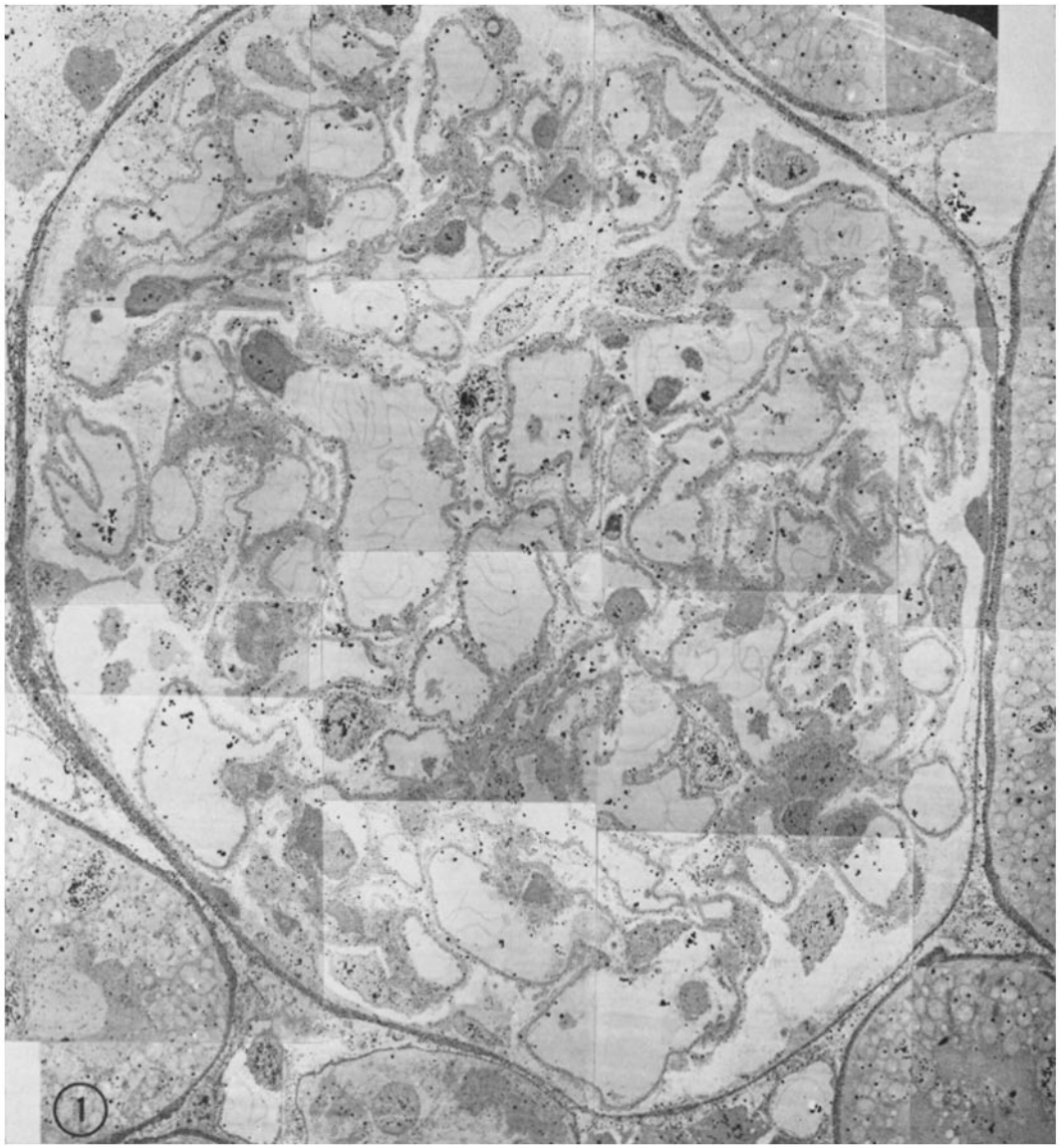

In all of these figures the kidneys have been fixed in saturated potassium pyroantimonate *alone* without addition of any conventional fixative, hardened with formaldehyde, postosmicated, and embedded in Maraglas. Staining was omitted, except for Figs. 8 and 9.

FIGURE 1 Survey electron micrograph of a thin section of rat kidney glomerulus illustrating its strikingly good preservation and the massive cation-antimonate precipitates in basement membranes at the boundary of glomerulus, glomerular capillary walls, proximal tubules, in the mesangium, in the interstitium, and in all cell nuclei. × 1180.

MATERIALS AND METHODS

Adult albino rats (Holtzman strain) were anesthetized with ether and perfused through the renal artery with the fixative at room temperature.

Electron Microscope Fixation Procedure

The fixative used was a saturated aqueous solution of potassium pyroantimonate (Riedel-De Haën Ag., Seelze, Hannover, Germany, analytical reagent) pre-

pared by boiling the salt in deionized or twice glass-distilled water, cooling rapidly to room temperature, and centrifuging (pH about 9.2). The pyroantimonate ion penetrates very quickly through the vasculature and the kidney becomes whitish almost instantaneously. The kidney was dissected free, minced into small pieces in a drop of the fixative, and thereafter immersed in a larger amount of the fixative for about 3 hr at room temperature.

The tissue was hardened in a formaldehyde-potassium pyroantimonate solution, washed with distilled water, and postosmicated as described before (2). Part of the tissue was heated in a half-saturated solution of potassium pyroantimonate after hardening with the formaldehyde solution (1), and postosmication was omitted.

Afterwards, the tissue was dehydrated with graded concentrations of cold ethanol, passed through propylene oxide, and embedded in Maraglas (The Marblette Co. Div. of Allied Products Corp., Long Island City, N.Y.). Thin sections were cut with glass knives on a Porter-Blum microtome, mounted on Formvar-coated copper grids (Belden Mfg. Co., Chicago, Ill.), and examined with a Siemens Elmiskop I electron microscope. The micrographs of Fig. 1 were taken with a Carl Zeiss EM9 A electron microscope.

Removal of Precipitates and Staining Procedure

Thin sections of pyroantimonate-fixed tissues stubbornly refuse to stain with the conventional uranyl acetate and lead citrate procedures (even at those sites which appeared free of precipitates). It was reasoned that this ought to be due to a "blocking" of the stainable sites by the pyroantimonate anion; therefore removal of this anion should allow the staining of pyroantimonate-fixed sections.

Tartaric acid is well known to solubilize antimony compounds due to the formation of complex ions; we have found oxalic acid much more effective in this respect. Addition of saturated oxalic acid to a saturated potassium pyroantimonate solution in a test tube causes the formation of a precipitate (due to the acid pH of the oxalic acid) which immediately redissolves. Similarly, the insoluble sodium and magnesium pyroantimonates readily dissolve in a saturated or half-saturated solution of oxalic acid; on the other hand, the pyroantimonate anion of the insoluble calcium (or zinc) salt is complexed with oxalic acid while the cation is reprecipitated as calcium (or zinc) oxalate.

When grids with the thin sections of pyroantimonate-fixed kidney were floated on a drop of saturated or half-saturated oxalic acid for 10–30 min at room temperature and thereafter washed with distilled water, it was observed that a large part of the electron-opaque deposits was indeed removed. Many of the precipitates leave an "empty" space at the sites where they were anchored. Furthermore, it was observed that not all precipitates were removed at the same velocity; probably those which are at, or near, the surface of the section dissolve more rapidly than those located deeper inside the Maraglas.

Simultaneous staining and removal of precipitates from the thin sections was found to be a reliable procedure by using a uranyl acetate–oxalic acid mixture. This solution is prepared by dissolving (at room temperature) oxalic acid crystals, up to saturation, in a saturated aqueous solution of uranyl acetate. Since oxalic acid is slowly decomposed by uranyl ions under the influence of light, the solution is stored in darkness. Staining is accomplished by floating the grids for 10–30 min on a drop of this solution, previously diluted with a small amount of distilled water (about 15:1) in order to prevent formation of precipitates. Since staining and removal of precipitates is a gradual process, it can be repeated several times (i.e. at short intervals) until a desirable contrast is obtained. After washing with distilled water, the grids are stained with lead citrate as usual.

RESULTS

Potassium Pyroantimonate as a Fixative

The most prominent features to be observed in *unstained*, postosmicated sections of kidney tissue perfused with potassium pyroantimonate are the excellent preservation of the over-all tissue and cell structures and the presence of abundant electron-opaque precipitates (Figs. 1–7). The general appearance of the glomerulus (Fig. 1) and proximal tubule (Fig. 6) does not vary significantly from that obtained after a conventional fixation (24): all of the major morphological features are

FIGURE 2 Same as Fig. 1, higher magnification, showing cation-antimonate precipitates in the basement membrane of the capillary walls and between the foot processes. *P*, podocyte; *M*, mesangium; *E*, endothelial cell. Scale mark, 1 μ. × 12,000.

FIGURE 3 Thin section through the juxtaglomerular apparatus. The precipitate is localized in the network of basement membrane material. The secretion granules are free of precipitate. *Nu*, nucleus; *E*, endothelium; *aa*, afferent arteriole; *P*, podocyte. Scale mark, 2 μ. × 5000.

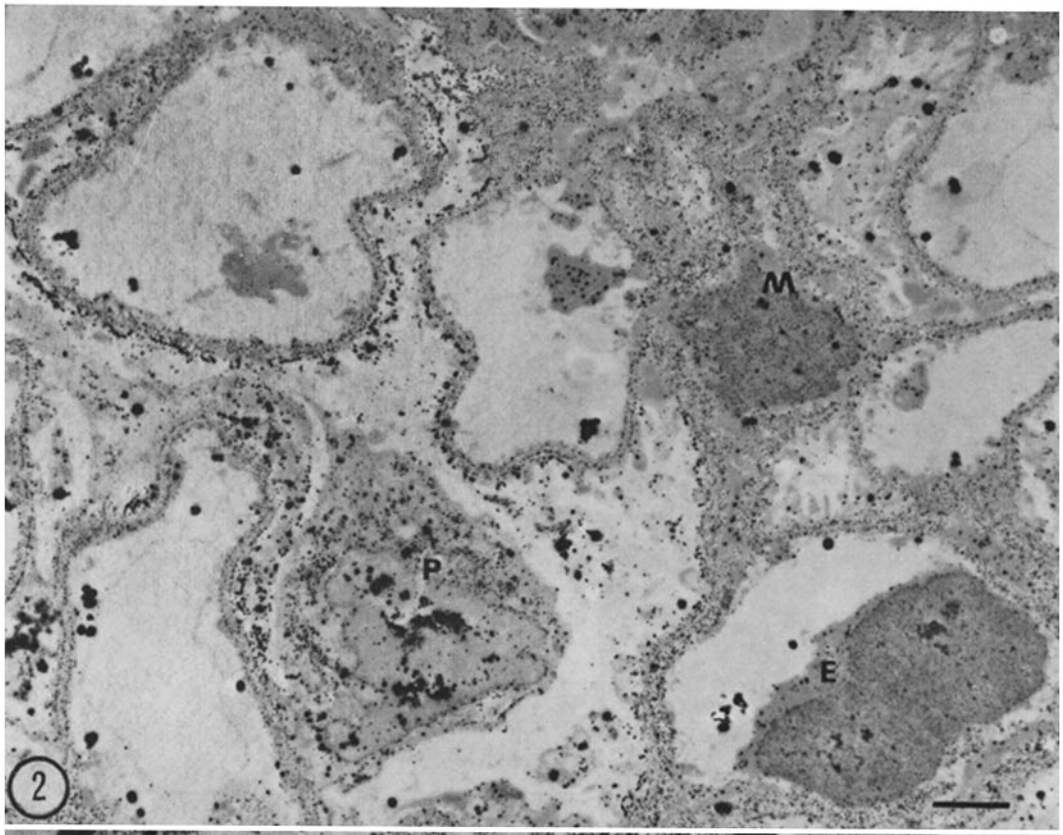
M
P
E
2

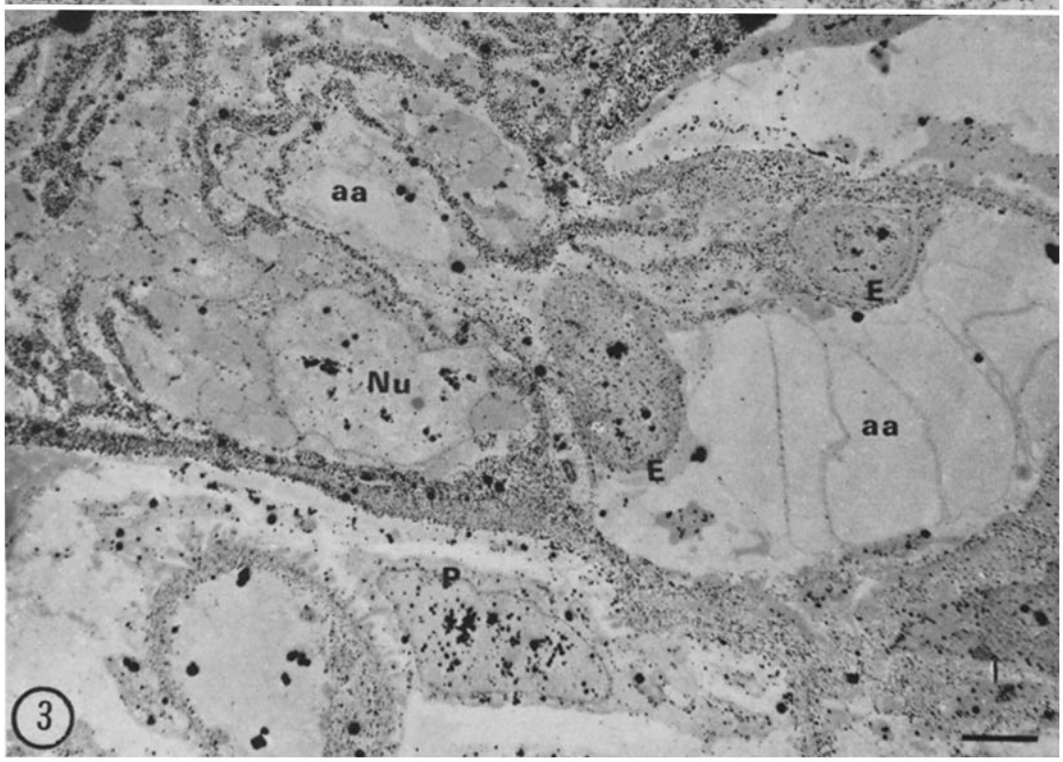
aa
E
Nu
aa
E
P
3

easily recognized. At higher magnifications, it can be seen that the integrity of cell membranes is well preserved (including those of mitochondria, Figs. 5 and 7, and the nuclear double membrane, Fig. 6).

Staining of thin sections and removal of antimonate precipitates with the oxalic acid–uranyl acetate mixture (followed by lead citrate) indicated a remarkably good preservation also at the ultrastructural level; thus, Figs. 8 and 9 compare well with the images obtained after a conventional aldehyde–osmium tetroxide fixation (24), except, of course, for the empty spaces left by solubilization of the precipitates. This evidence conclusively demonstrates that potassium pyroantimonate is a *good fixative*. In addition it "fixes"—by precipitation—a number of inorganic cations (1, 2), a property which makes this salt a suitable histochemical reagent.

The electron-opaque precipitates were also evidenced after heating the pyroantimonate-fixed tissues in a half-saturated potassium pyroantimonate solution, suggesting that they were not formed by deposition of the fixative itself but rather by a precipitation reaction with the tissue cations (mainly magnesium, calcium, and sodium, 1, 2). The elementary scanning of thick (1-μ) sections with the electron microprobe (performed by Dr. C. M. Libanati of the Commission of Atomic Energy) showed the presence of those inorganic cations in the antimonate deposits, in accordance with the results obtained with pyroantimonate-fixation in other tissues (1, 2).

Pattern of Cation-Antimonate Precipitation

The distribution of the cation-antimonate deposits was found to be a constantly reproducible result in all of the kidneys examined. All proximal and distal tubules (Figs. 6 and 1) and the glomerulus (Fig. 1) are delimited by heavy cation-antimonate precipitates localized in the basement membrane and, to a lesser extent, in adjacent connective tissue. The same thing happens around all of the small blood vessels in the interstitium (Fig. 1) and in the network of basement membrane–like (24) material of the juxtaglomerular apparatus (Fig. 3).

The normal appearance of the basement membranes and collagen fibrils after pyroantimonate fixation is evidenced in Fig. 9, where the larger part of the antimonate precipitates was dissolved by oxalic acid and stained by uranyl oxalate and lead citrate. Furthermore, it can be seen that some electron-opaque precipitates remained undissolved and that these were indeed located within the basement membrane of Bowman's capsule (Fig. 9).

Variable amounts of electron-opaque deposits are present in all nuclei; at higher magnifications many of them are seen as spherical granules or granular aggregates (Figs. 2, 3, and 6) similar in appearance to those found in the nuclei of other tissues (1, 2). This type of precipitate is anchored between the masses of condensed chromatin as indicated by extraction of the antimonate precipitates with oxalic acid: the condensed chromatin takes the uranyl and lead stains while the sites of antimonate deposits appear as empty spaces (Fig. 9).

The mitochondria usually contain a few electron-opaque granules (Figs. 5–7); that they really lie inside the mitochondria is evident from Fig. 7 where one such granule has been displaced by the microtome knife (during the sectioning) and leaves an empty space.

FIGURE 4 Electron micrograph showing three confluent glomerular capillary walls with the precipitate located in the basement membrane and more concentrated at the area of contact with the foot processes. *P*, podocyte. Scale mark, 0.5 μ. × 21,000.

FIGURE 5 Electron micrograph illustrating the appearance of cation-antimonate precipitates between foot processes of the podocyte. *m*, mitochondria; *bm*, tangential section through the basement membrane of the capillary wall. Scale mark, 0.25 μ. × 30,000.

FIGURE 6 Thin section through part of a proximal tubule showing the antimonate precipitates in the basement membrane (*bm*), cytoplasm and within the nucleus (*Nu*). A few larger deposits are present in the mitochondria. *E*, endothelial cell. Scale mark, 0.5 μ. × 15,000. *Insert:* thin section through a portion of the apical cytoplasm showing antimonate precipitates along the microvilli. Scale mark, 0.25 μ. × 22,000.

FIGURE 7 Same as Fig. 6, higher magnification, showing large, spherical antimonate deposits within the mitochondria; one of them has been displaced by the microtome knife, leaving an empty space (arrow). *bm*, basement membrane. Scale mark, 0.2 μ. × 37,500.

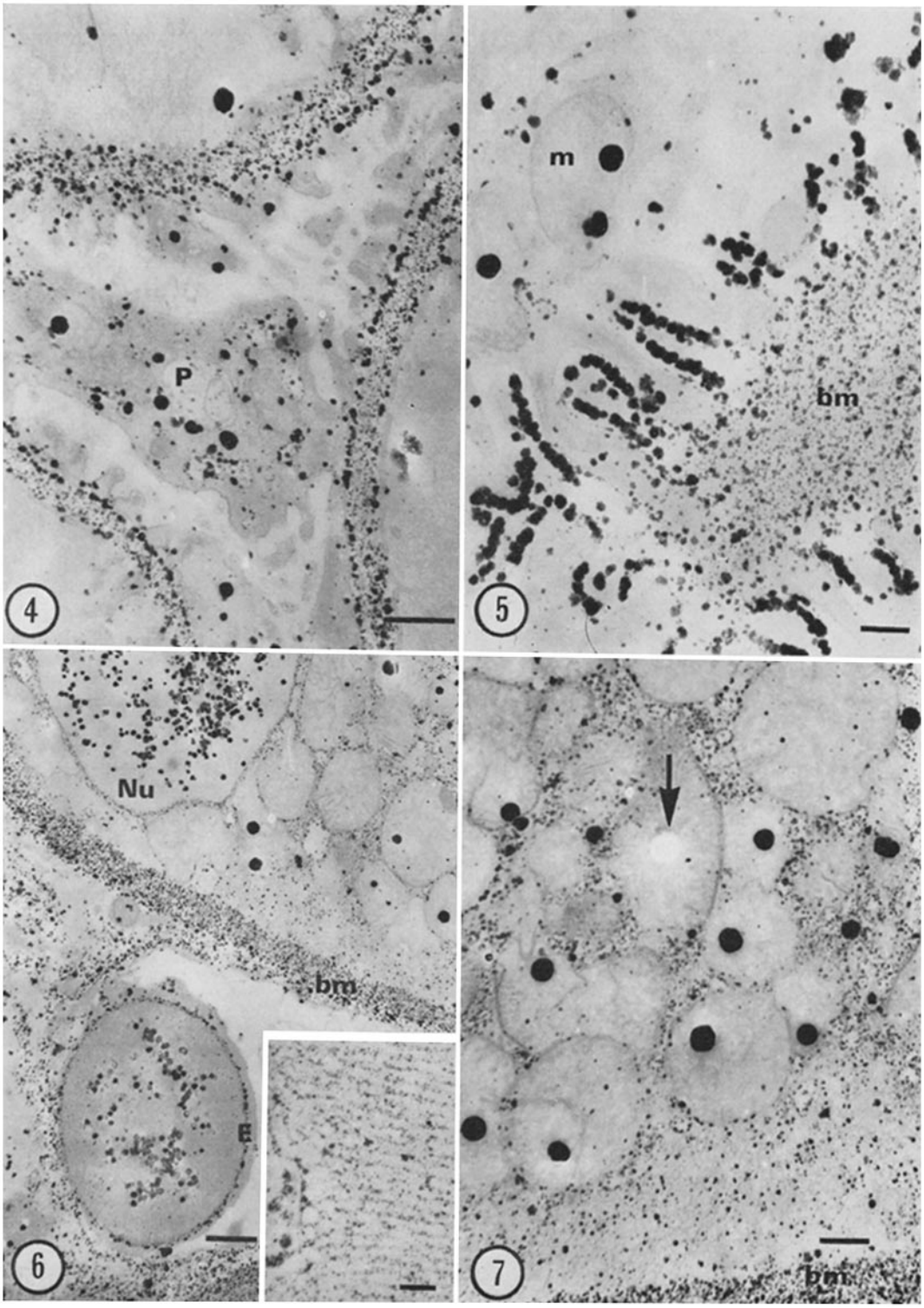
P
4
m
bm
5
Nu
bm
6
7
bm

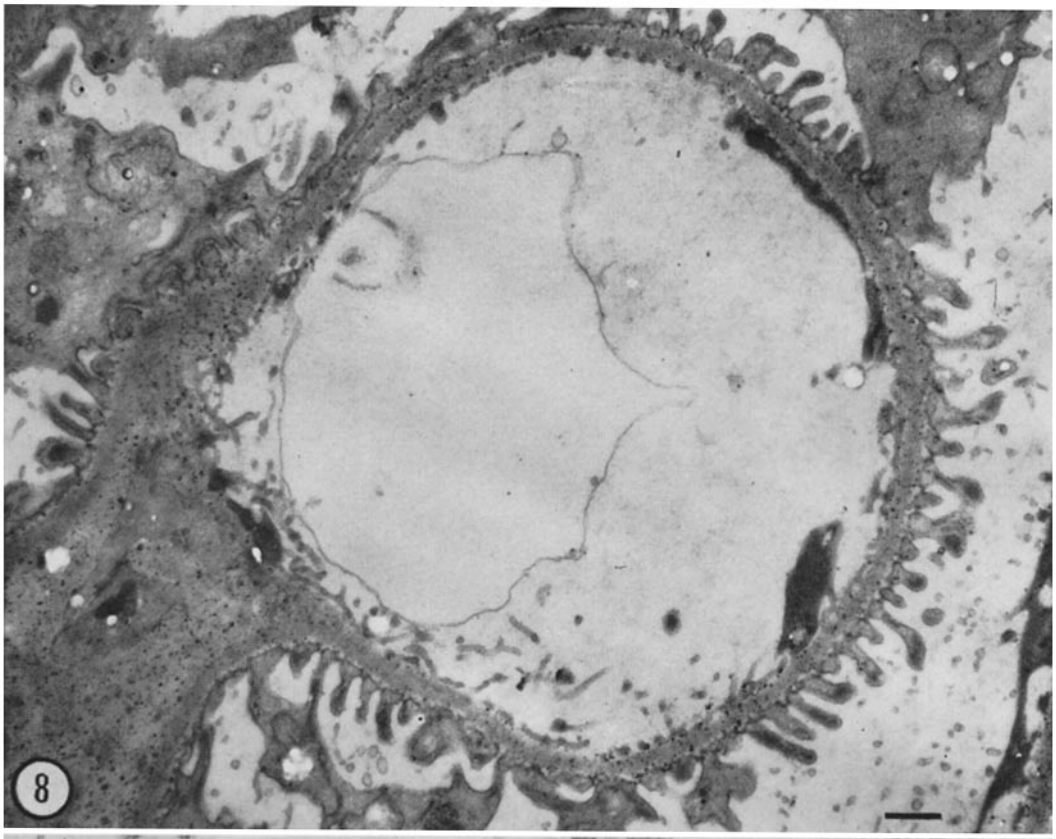

8

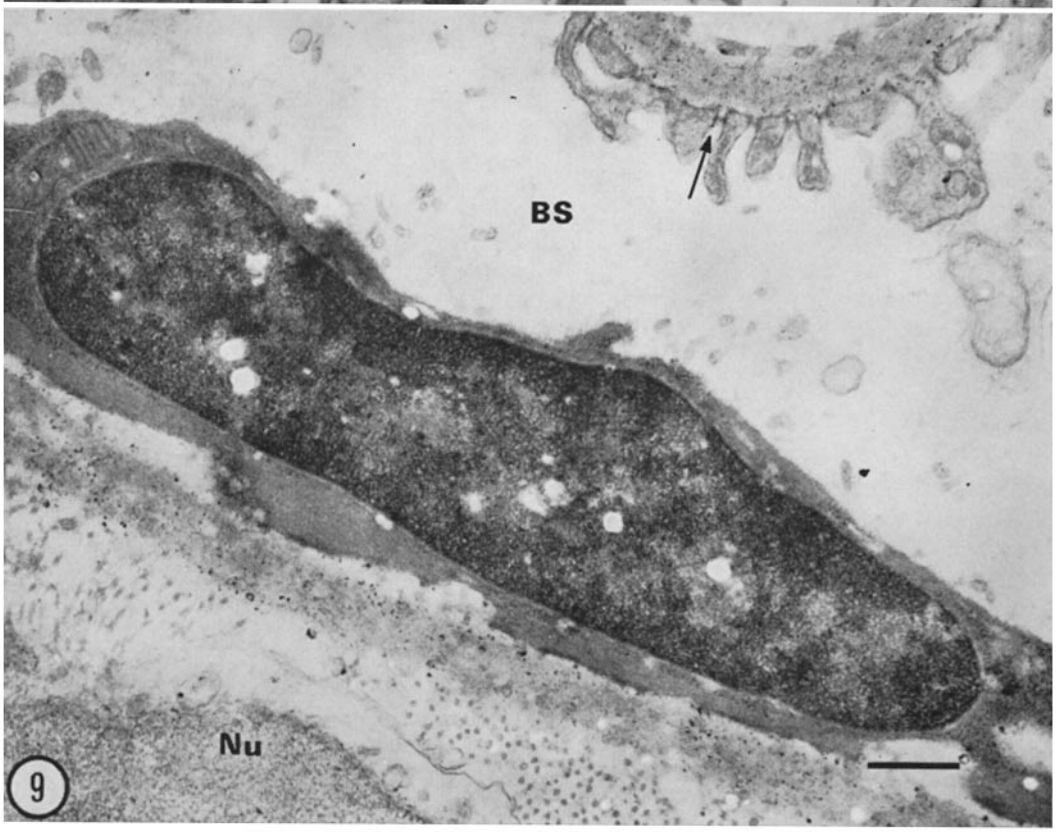

9

The Glomerulus

Electron-opaque precipitates are found in the capillary walls of the glomerulus (Figs. 1 and 2). At higher magnifications it can be seen that the thin extended cytoplasm of the endothelium is relatively free of precipitate (Fig. 4); the fenestrations described after conventional fixations (24, 25) are also preserved after pyroantimonate fixation (Fig. 4; and after uranyl oxalate staining, Fig. 8). The antimonate precipitate is encountered in the region where the nucleus of an endothelial cell projects into the lumen of the vessel (including the cytoplasm of the cell) and in the mesangium (Fig. 2).

The larger part of the antimonate precipitates in the glomerular capillary walls is located in the zone occupied by the basement membrane; it appears frequently concentrated—in the form of larger granules—at the area of contact of the basement membrane and both the endothelial lining (Figs. 2 and 4) and the foot processes of the podocytes (Fig. 4). In the rat the substance of the basement membrane is more concentrated at the center of the space delimited by the endothelium and the epithelial foot processes (26), and this morphology is maintained after pyroantimonate fixation as demonstrated by uranyl oxalate and lead citrate staining (Fig. 8). In this compact central layer of the basement membrane the antimonate precipitate is frequently more finely granular than in the other layers (Fig. 2). In Fig. 4, a heavy line of granules of antimonate precipitate is seen accumulated between the plasma membrane of the foot processes and the central compact layer of the basement membrane. At some other places this type of granular precipitate appears concentrated between and on the foot processes (Fig. 5).

As demonstrated in uranyl oxalate–extracted and stained sections—followed by lead staining—the spatial relationships between endothelium, basement membrane, and foot processes are well preserved by pyroantimonate fixation; at many places the slit between the foot processes is also discernible (Fig. 8). Furthermore, it can be seen that some precipitates remain undissolved and that these are located within the basement membrane of a glomerular capillary and in the mesangium as well.

DISCUSSION

The main point demonstrated here—together with the evidence presented in previous papers (1, 2)—is that potassium pyroantimonate *alone*, without the addition of any conventional fixative, resulted in a strikingly good preservation of tissue and cell morphology and a prominent precipitation of the insoluble antimonate salts of magnesium, calcium, and sodium. In the kidney the localization pattern of the cation-antimonate deposits was essentially the same when the immersion and perfusion fixations were compared; with the latter procedure, besides a much better morphological preservation, the antimonate precipitates were usually finer, more abundant, and uniformly granular.

Among the loci showing electron-opaque precipitates, those of the basement membranes and the cell nuclei (Figs. 1–3, and 6) were predictable on the basis that they showed similar reactivity in mouse testis (2), rat liver (1), and (for the nuclei) in plant material (1). Moreover, since other tissues tested recently, i.e. rat ovary (Schuchner and Tandler, in preparation) and a human basal cell carcinoma (Kierszenbaum and Tandler, in preparation), behaved similarly, it is very likely that the existence of a relatively high level of inorganic cations is a general property of all basement membranes (extending somewhat over regions of connective tissue closely associated

FIGURE 8 Thin section through a glomerular capillary illustrating the good preservation at the ultrastructural level. The antimonate precipitates have been removed almost completely with oxalic acid; many of them have left an "empty" space. Some fine precipitate has remained in the basement membrane and in the mesangium. Stained with uranyl oxalate and lead citrate. Scale mark, 0.2 μ. × 35,000.

FIGURE 9 Same as Fig. 8, showing the empty spaces located between the masses of condensed chromatin in the nucleus of an epithelial cell of Bowman's capsule. Some fine precipitate remained in the basement membrane of the capsule and of a glomerular capillary wall; the slit membrane connecting the foot processes is discernible (arrow). *BS*, Bowman's space; *Nu*, nucleus of a fibroblast. Stained with uranyl oxalate and lead citrate. Scale mark, 0.2 μ. × 60,000.

with them). As for the cell nucleus, the distribution of inorganic cations is not uniform since the condensed chromatin has been shown to be relatively free of antimonate-precipitable cations (1, 2).

The large antimonate deposits found in mitochondria (Figs. 5–7) probably correspond to the dense granules (24, 25, 27) observed after the conventional fixation and staining procedures and identified, mainly, as precipitates of calcium and magnesium phosphates (25, 27). After pyroantimonate fixation the electron opacity of the intramitochondrial granules is much heavier, suggesting their conversion into insoluble calcium and magnesium pyroantimonates. However, further evidence is needed to ascertain the identity of the dense bodies preserved after both types of fixations.

Previous studies on rat kidney were based on the formation of electron-opaque deposits with the use of fixation in osmium tetroxide–potassium pyroantimonate mixtures (9, 13, 18). The method used in the present paper has the advantage that the precipitating reagent itself behaves as a fixative; in this manner the effect of any combination of conventional fixative plus the precipitating reagent can be evaluated separately. In general, after these mixed fixatives the antimonate precipitates were much less abundant than after fixation in potassium pyroantimonate alone, indicating leakage of cations by the conventional fixative, a finding observed in other tissues (1, 2).

A possible interference with pyroantimonate fixation procedures is indicated by the solubilization of cation-antimonate precipitates by certain organic acids such as oxalic acid, as described above; citric and ascorbic acid were found to behave similarly in the test tube. Since this effect occurs at an acid pH, the relatively high pH of the potassium pyroantimonate solution employed (about 9.2) might be important in minimizing that interference.

The present paper presents evidence—for the first time at the electron microscope level, we think—on the localization of inorganic cations in the glomerulus and in the juxtaglomerular apparatus. Their distribution in the glomerulus, indicated by the pattern of antimonate precipitation of Fig. 1, is very similar to the localization of minerals obtained by Scott (28) after microincineration of frozen-dried kidney sections; he also presented the emission electron image of calcium plus magnesium in his incinerated sections and found these elements to be present around the glomerular capillaries and the Bowman's capsule and in the cell nuclei as well.

The use of the electron microscope to study the pathways followed by electron-opaque tracers during their passage through the capillary wall has indicated that the mode of transport may vary with the kind of material being transported. These variations, obtained with small proteins and colloidal particles, with larger globin aggregates, and during hemoglobin excretion (26), have been reviewed recently (29). The evidence presented here indicates that the small cations pass between epithelial foot processes on their way from the basement membrane to Bowman's space.

It is interesting that, within a given section, the presence of the precipitate between the foot processes is not associated with all capillaries (Fig. 1). This could be due to the section incidence or, alternatively, it could be that the process of filtration is not simultaneous (or continuous) in all of the capillaries. The flow of ions through the basement membrane and through the polysaccharide extraneous coat (30) of the podocyte processes could be two different steps requiring different periods of time for completion. It is also probable that these loci bind inorganic cations strongly and could act, due to the positive charge of the cations, as a "barrier" to cation transport.

This investigation was supported in part by the Dirección Argentina Filantrópica Asistencial de Citología del Cancer (DAFACC). Dr. Tandler is an established Investigator of the Consejo Nacional de Investigaciones Científicas y Técnicas, Argentine.

Received for publication 28 December 1970, and in revised form 22 February 1971.

REFERENCES

1. TANDLER, C. J., C. M. LIBANATI, and C. A. SANCHIS. 1970. *J. Cell Biol.* **45**:355.
2. KIERSZENBAUM, A. L., C. M. LIBANATI, and C. J. TANDLER. 1971. *J. Cell Biol.* **48**:314.
3. TANDLER, C. J., and A. J. SOLARI. 1969. *J. Cell Biol.* **41**:91.
4. LIBANATI, C. M., and C. J. TANDLER. 1969. *J. Cell Biol.* **42**:754.
5. KOMNICK, H. 1962. *Protoplasma.* **55**:414.
6. KOMNICK, H., and U. KOMNICK. 1963. *Z. Zellforsch. Mikrosk. Anat.* **60**:163.
7. KAYE, G. I., J. D. COLE, and A. DONN. 1965. *Science (Washington).* **150**:1167.
8. KAYE, G. I., H. O. WHEELER, R. T. WHITLOCK, and N. LANE. 1966. *J. Cell Biol.* **30**:237.

9. NOLTE, A. 1966. *Z. Zellforsch. Mikrosk. Anat.* **72:** 562.
10. ZADUNAISKY, J. A. 1966. *J. Cell Biol.* **31:**C11.
11. HARTMANN, J. F. 1966. *Arch. Neurol.* **14:**633.
12. SPICER, S. S., J. H. HARDIN, and W. B. GREENE. 1968. *J. Cell Biol.* **39:**216.
13. BULGER, R. E. 1969. *J. Cell Biol.* **40:**79.
14. LEGATO, M. J., and G. A. LANGER. 1969. *J. Cell Biol.* **41:**401.
15. LANE, B. P., and E. MARTIN. 1969. *J. Histochem. Cytochem.* **17:**102.
16. HARDIN, J. H., S. S. SPICER, and W. B. GREENE. 1969. *Lab. Invest.* **21:**214.
17. SIEGESMUND, K. A. 1969. *J. Anat.* **105:**403.
18. TISHER, C. C., W. J. CIRKSENA, A. U. ARSTILA, and B. F. TRUMP. 1969. *Amer. J. Pathol.* **57:** 231.
19. VINNIKOV, Y. A., and K. KOICHEV. 1969. *Nature (London).* **223:**641.
20. HARDIN, J. H., and S. S. SPICER. 1970. *J. Ultrastruct. Res.* **31:**16.
21. TORACK, R. M., and M. LA VALLE. 1970. *J. Histochem. Cytochem.* **18:**635.
22. SHIINA, S., V. MIZUHIRA, T. AMAKAWA, and Y. FUTAESAKU. 1970. *J. Histochem. Cytochem.* **18:** 644.
23. SATIR, P., and N. B. GILULA. 1970. *J. Cell Biol.* **47:**468.
24. DALTON, A. J., and F. HAGUENAU, editors. 1967. Ultrastructure of the Kidney. Academic Press Inc., New York.
25. PORTER, K., and M. A. BONNEVILLE. 1968. Fine Structure of Cells and Tissues. Lea and Febiger, Philadelphia, Pa.
26. LATTA, H. 1970. *J. Ultrastruct. Res.* **32:**526.
27. LEHNINGER, A. L. 1964. The Mitochondrion. Molecular Basis of Structure and Function. W. A. Benjamin Inc., New York.
28. SCOTT, G. H. 1943. *Biol. Symp.* **10:**284.
29. MENEFEE, M. G., and C. B. MUELLER. 1967. *In* Ultrastructure of the Kidney. A. J. Dalton and F. Haguenau, editors. Academic Press Inc., New York. 73.
30. GRONIOWSKI, J., W. BICZYSKOWA, and M. WALKSI. 1969. *J. Cell Biol.* **40:**585.